

Photoacoustic detection of stimulated emission pumping in *p*-difluorobenzene^{a)}

D. J. Moll,^{b),c)} G. R. Parker, Jr.,^{d)} and A. Kuppermann

Arthur Amos Noyes Laboratory of Chemical Physics,^{e)} California Institute of Technology, Pasadena, California 91125

(Received 21 September 1983; accepted 8 December 1983)

Photoacoustic detection has been used to monitor a stimulated emission pumping process in *p*-difluorobenzene. Using the $\tilde{A}^1B_{2u}5^1$ state as an intermediate, several vibrational levels of the ground electronic state were populated. The photoacoustic method is an attractive alternative to other detection techniques because of its sensitivity, simplicity, and its ability to differentiate between stimulated emission pumping and excited state absorption. An example of excited state absorption in aniline is given.

I. INTRODUCTION

Stimulated emission pumping (SEP) has recently been demonstrated as a powerful technique for selectively preparing large numbers of molecules in specific highly excited rovibrational states of the ground electronic state for diatomic or small polyatomic molecules.¹⁻⁵ The SEP process produces this selective vibrational excitation as a result of two sequential steps. First a PUMP laser excites molecules from an initial level 1 of the ground electronic state to a level 2 in an excited electronic state. Then, a DUMP laser stimulates emission out of this excited state to a lower energy state, level 3, resulting in an overall excitation from level 1 to level 3. SEP therefore provides an alternative excitation route that may be much more efficient in some cases than direct excitation.

SEP is especially attractive for producing large populations in specific high vibrational states of the ground electronic state. It often allows the substitution of favorable Franck-Condon factors and easily obtainable tunable visible or UV lasers for weak $|\Delta v| > 1$ vibrational transitions and difficult to obtain tunable IR lasers. In formaldehyde, for example, it was estimated that $> 0.02\%$ of the total thermal population within the PUMP beam was excited to a specific rotational level in the $\nu_4 = 4$ vibrational state by an SEP process.³

This paper describes the use of the photoacoustic effect for detecting the SEP process in a specific molecule, *p*-difluorobenzene (*p*-DFB). This technique permits a determination of the total energy remaining in the molecule after applying the PUMP and DUMP pulses. It is therefore possible to establish whether the DUMP pulse stimulates emission out of level 2 (SEP) or results in an excited state absorption (ESA).

II. PREVIOUS SEP DETECTION TECHNIQUES

Two techniques have previously been used to monitor the SEP process. Kittrel *et al.*¹ and Reisner *et al.*³ in their

studies of SEP in I₂ and formaldehyde, respectively, monitored the change in fluorescence from level 2 (an excited singlet state) as a function of the DUMP pulse wavelength (see scheme I of Fig. 1). The transition from level 2 to level 3 stimulated by the DUMP pulse results in a decrease of the intensity of the fluorescence out of level 2. This technique is relatively uncomplicated and benefits from the high sensitivity of fluorescence detection techniques. One disadvantage of this scheme arises from its sensitivity to processes other than the stimulation of emission which could also decrease the detected fluorescence intensity. For example, the excited state produced by the PUMP pulse could absorb DUMP photons (instead of being stimulated to emit), resulting thereby in an excitation of the molecule to higher electronic states which rapidly predissociate or autoionize. This additional excitation process would effectively decrease the observed fluorescence intensity. For the case of I₂ and formaldehyde, the spectroscopic evidence clearly supports the almost exclusive occurrence of SEP. However, attempts to observe SEP processes involving the \tilde{A}^1B_2 state of aniline (see Sec. V) strongly indicate the presence of up-pumping by the "DUMP" pulse to autoionizing or predissociative states which competes effectively with stimulating emission back to the ground electronic state.⁸ Therefore, without a prior detailed knowledge of the spectroscopy of the molecule to be investigated and careful investigation of other possible fluorescence-decreasing processes, the fluorescence detection technique could give misleading results.

A second method of monitoring the SEP process was employed by Lawrence and Knight^{2,4,5} (see scheme II of Fig. 1). They demonstrated SEP as an effective method for populating vibrational levels of the ground electronic state in a medium-sized polyatomic molecule, *p*-DFB,² and used the SEP process as a preparative method to produce specific vibrational states whose lifetimes were measured.^{4,5} In those experiments the standard PUMP and DUMP pulses were followed by a third pulse, the PROBE pulse of a laser induced fluorescence (LIF) detection scheme.^{6,7} This technique offers the advantage of specific detection of the level populated by SEP, rather than assuming that a decrease in fluorescence intensity corresponds to the preparation of a specific vibrational state. The possibility of partial absorption of the DUMP pulse and further excitation is not eliminated, but by monitoring the population of the final vibrational

^{a)} Research supported in part by the U.S. Department of Energy, (Contract No. DE-AS03-76F00767, Project Agreement No. DE-AT-76ER72004).

^{b)} Work performed in partial fulfillment of the requirements for the Ph.D. degree in Chemistry at the California Institute of Technology.

^{c)} Current address: Dow Chemical Company, Midland, MI 48640.

^{d)} NSF predoctoral fellow.

^{e)} Contribution No. 6913.

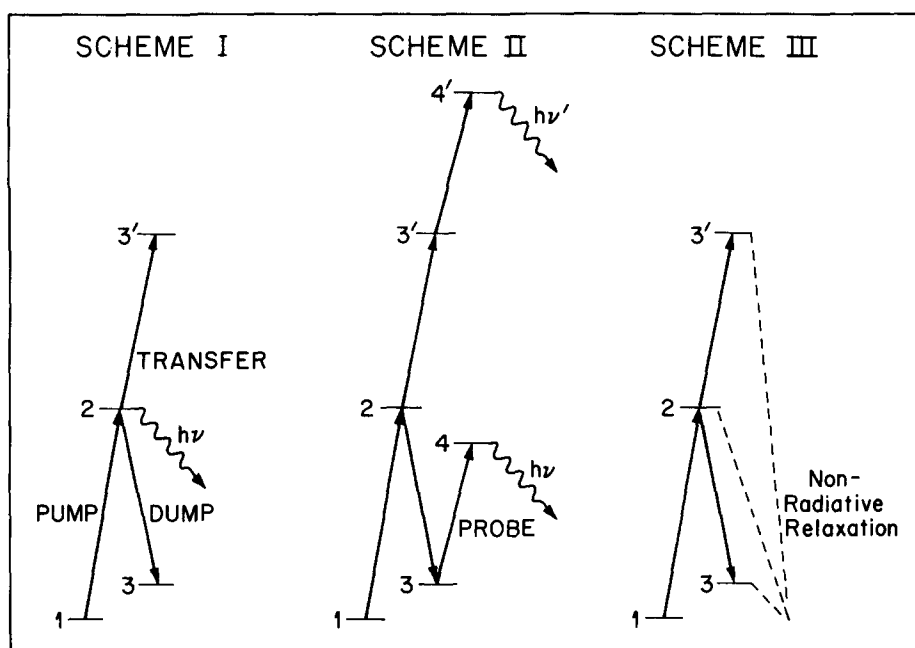


FIG. 1. Schemes for detecting stimulated emission and absorption.

state, the extent of the stimulated emission process is directly observed. The major disadvantage of this technique is the complexity of obtaining and overlapping three different laser pulses, both temporally and spatially. In addition, the spectroscopy of the molecule being studied must be known sufficiently well to allow selection of an appropriate wavelength for the PROBE laser.

The pulsed photoacoustic detection method (scheme III of Fig. 1) functions as follows. As photons from a nanosecond laser pulse are absorbed by the sample, they result in excitation of its molecules. The excited molecules can then relax by either radiative or nonradiative pathways. The latter results in an increase in pressure in the sample, which propagates as a pressure wave to the microphone detector. The traversal time of this pressure wave is of the order of a few tens of microseconds. For excitation of a given state of the molecule, the intensity of the microphone response signal increases with the number of molecules produced in that state.

The PUMP pulse alone in the present experiments excites the sample molecules to level 2. The molecules in this state which relax nonradiatively result in the pressure wave detected by the microphone. When the DUMP pulse stimulates transition from level 2 to level 3, the detector signal due to level 2 decreases. In general, the signal intensity produced by a molecule in level 3 is smaller than that produced by a molecule in level 2 because its excitation energy is much less. Under these circumstances, the net signal detected after application of both the PUMP and DUMP pulses is smaller than that after the PUMP pulse alone.

If on the other hand, the DUMP pulse is absorbed, the resulting level 3' has a significantly higher energy than that of level 2 and is apt to produce a larger microphone response than level 2. Under these conditions, the net signal after application of both the PUMP and DUMP pulses is greater than that after the PUMP pulse alone. Therefore, by monitoring the increase or decrease in photoacoustic signal when

the DUMP pulse immediately follows the PUMP pulse, compared to the PUMP pulse alone, it is usually possible to differentiate between excited state absorption and stimulated emission. Assuming thermalization of the molecule formed by nonradiative processes, the extent of the effect can be estimated if the relative quantum yields for nonradiative processes from the excited states are known. The ability to differentiate between absorption and stimulated emission provides a distinct advantage over the simple fluorescence detection method. The simplicity of the photoacoustic detection method makes it an attractive alternative to the LIF detection scheme.

III. EXPERIMENTAL

The time-resolved two-color photoacoustic measurement involved in monitoring SEP described in this paper is a new application of photoacoustic spectroscopy. This same technique is also applicable to gas phase excited state absorption measurements with nanosecond or faster time resolution.⁸ (We believe this to be the first gas phase nanosecond timescale photoacoustic spectroscopy measurements. Previous experiments have involved solid^{9(a)} and solution^{9(b),9(c)} phase samples).

A. Lasers and optics

The experimental arrangement is depicted in Fig. 2. It consists of two counter-propagating collinear beams from frequency doubled dye lasers which pass through a photoacoustic cell containing *p*-DFB. The PUMP pulse is generated by dye laser # 1, a Molelectron¹⁰ DL200 dye laser pumped by a Molelectron UV400 N₂ laser. The dye laser output was frequency doubled in a potassium dihydrogenphosphate (KDP) crystal (C2), collimated with a 25 cm focal length lens (L3), and directed into the photoacoustic cell. Using Coumarin 485 dye in ethanol, typical UV pulse energies at the photoacoustic cell entrance were $\sim 15 \mu\text{J}$. The DUMP pulse

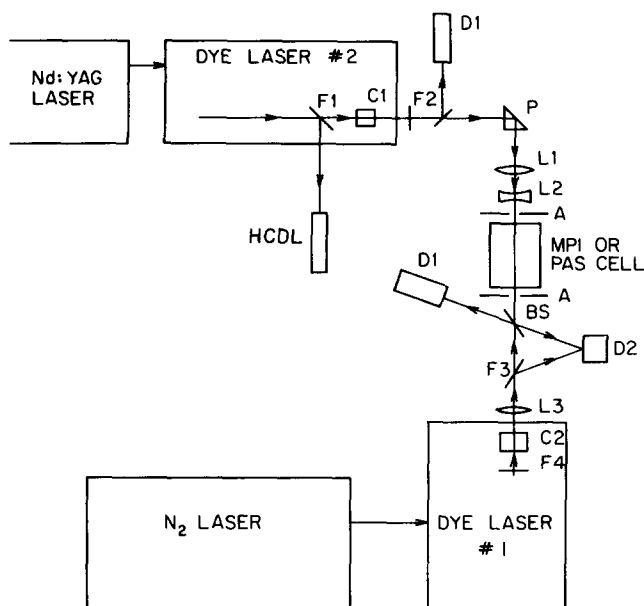


FIG. 2. Experimental arrangement for photoacoustic detection of stimulated emission. The PUMP beam from dye laser #1 and the DUMP beam from dye laser #2 enter a photoacoustic cell collinearly from opposite directions. The various labels are defined as follows: A—aperture, BS—beam splitter, C1 and C2—KDP doubling crystals, D1—pyroelectric energy probe, D2—high speed photodiode, F1 and F4—UV blocking filters, F2 and F3—UV pass filters, HCDL—uranium/neon hollow cathode discharge lamp, L1 and L2—beam contracting telescope, L3—25 cm focal length lens, P—prism.

is generated by dye laser #2, a Molectron DL18 dye laser including an oscillator and a single longitudinally pumped amplifier, pumped by a Molectron MY34 Nd:YAG laser. The output of dye laser #2 is also doubled in a KDP crystal (C1) and directed into the opposite end of the photoacoustic cell. A beam contracting telescope (L1, L2) is used to match the beam diameters of the two frequency-doubled dye laser outputs (~ 1 mm). Using rhodamine 6G (R6G) dye in ethanol, typical UV pulse energies before entering the photoacoustic cell are between 2 and 10 mJ. UV outputs from either dye laser were monitored off beam splitters with a Laser Precision¹¹ pyroelectric joulemeter, model RkP-335, and readout unit, model Rk-3230. The analog output from the readout unit was processed by a differential gated integrator system described later.

Initial experiments indicated that the two dye lasers interacted with each other due to the collinear counter-propagating beam arrangement. This was eliminated by using Corning 7-54 UV pass filters to block the visible output after each doubling crystal, and Corning 0160 glass before each doubling crystal to keep the UV produced by one laser from entering the other.

Wavelength scans of either dye laser are achieved using microcomputer controlled stepping motors to drive the gratings. The phase matching angle for the doubling crystal of dye laser #1 is adjusted manually during wavelength scans. The crystal for dye laser #2 is controlled by the microcomputer. Wavelengths were calibrated using a uranium/neon hollow cathode discharge lamp (HCDL) and the optogalvanic effect.¹² UV output linewidths were ≤ 1 cm⁻¹.

B. Photoacoustic cell

Photoacoustic spectroscopy and the design of photoacoustic cells has been recently reviewed.^{13,14} The photoacoustic cell used in this study is similar to that of West *et al.*¹⁵ An 18 cm long by 0.9 cm diameter cell was constructed of stainless steel and aluminum and had quartz windows at each end. Since extreme sensitivity was not essential in working with the strong absorptions in *p*-DFB the cell was designed to minimize signals arising from scattered light striking the microphone or cell walls. Since most light scattering occurs at the windows, this is achieved by a series of apertures both inside and outside the cell. The microphone, Knowles Electronics¹⁶ BT1759, is located 6 cm away from the PUMP pulse entrance window rather than at the middle of the cell in order to decrease absorption of that pulse before it reaches the vicinity of the microphone. The microphone is positioned over 3/16 in. diameter hole in the cell wall and held in place with epoxy resin.

C. Timing and data acquisition electronics

The timing and data acquisition electronics are depicted schematically in Fig. 3. The time delay between laser pulses is controlled by three pulse generators. Pulse generator A is triggered by the 10 Hz Nd:YAG flashlamp synchronization output and generates most of the 150 μ s delay before the YAG Q-switch normally fires. After this initial delay, two fast risetime pulse generators (B and C) are used to independently trigger the N₂ laser thyatron and the Nd:YAG Q-switch.

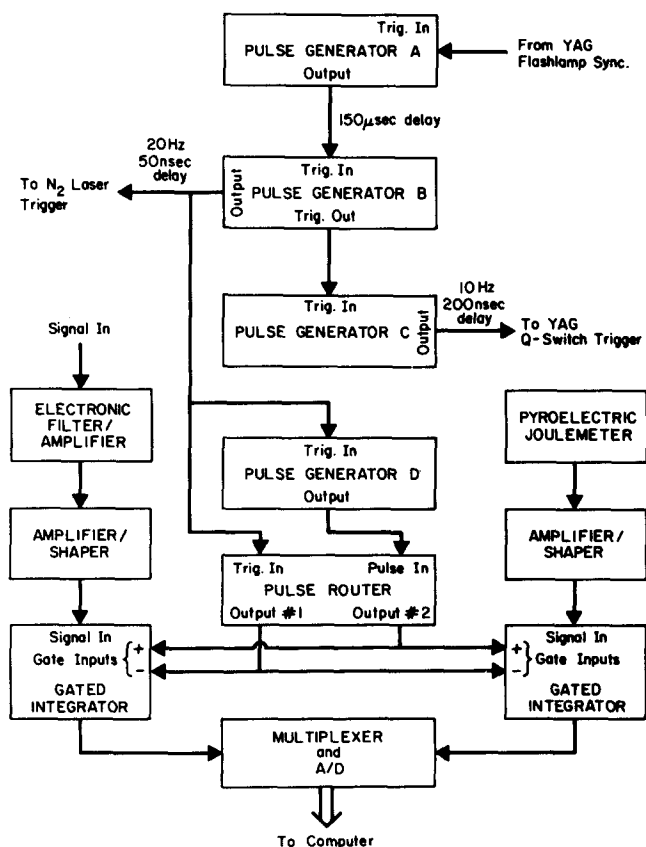


FIG. 3. Schematics of the electronics for a wavelength scan.

The time delay is monitored with a Hewlett Packard 5082-4220 PIN photodiode (-18 V bias, $\tau_{\text{rise}} < 1$ ns) and a 10 ns rise time oscilloscope. Long term jitter between pulses is less than ± 2 ns, while short term jitter is only ± 1 ns. The pulsewidth of the frequency-doubled output of each laser is < 5 ns.

Signals from the photoacoustic cell are limited to a frequency range of 0.1 to 80 kHz by an electronic filter and are then amplified. The peak of the first pressure wave of the photoacoustic signal is integrated by a differential gated integrator system with an integration window of $15 \mu\text{s}$. These integration windows are generated by pulse generator D.

In some experiments the time delay is scanned. This is accomplished by attaching a 1 revolution/h synchronous motor to the vernier delay knob of pulse generator B. In these experiments, the integrator measures the difference between the photoacoustic signal and the background.

In other experiments the DUMP pulse wavelength is scanned. In these experiments, pulse generator B is operated in a double pulse mode, firing the N_2 laser twice for each time the Nd:YAG fires. The integrator in this case measures the difference in photoacoustic signal between that from the PUMP plus DUMP pulses and that from the PUMP pulse alone. This is accomplished with the help of a pulse router circuit.

In both types of experiments, a second integrator system is used to measure the energy of the DUMP pulses. The output of both integrators is digitized and then stored on a floppy disk for later analysis.

D. Sample preparation

p-DFB was obtained from the Aldrich Company and had a normal purity of 98%. It was subjected to several liquid N_2 freeze-pump-thaw cycles and vacuum distilled on a

vacuum line operated at 5×10^{-7} Torr pressure. Sample pressures ranged from 0.020 to 0.060 Torr as measured by a Baratron. At the lower sample pressures helium was sometimes added to increase the photoacoustic signal through enhanced collisional relaxation. This had no effect on the fractional change in the signal resulting from the SEP process.

Aniline was used to obtain an absorption spectra of an electronically excited state (see Sec. V). This substance was obtained from Mallinckrodt Inc., subjected to several freeze-pump-thaw cycles and vacuum distilled as above. The samples were stored in the dark. After filling the photoacoustic cell with the sample, its pressure was allowed to stabilize for several minutes before closing the cell valve to minimize the effect of wall absorption.

IV. STIMULATED EMISSION PUMPING IN *p*-DIFLUOROBENZENE

We chose *p*-DFB to demonstrate the effectiveness of photoacoustic detection for monitoring SEP because of its extensively studied absorption and emission spectra and to allow comparison with previous SEP studies of the same molecule.^{2,4,5}

A. Background

Infrared,¹⁷ Raman,¹⁷ and two-photon¹⁸ studies have previously been used to determine the ground state (\tilde{X}^1A_{1g}) vibrational frequencies of *p*-DFB. The S_1 (\tilde{A}^1B_{2u}) excited state vibrational frequencies have also been previously determined.¹⁸⁻²² Single vibronic level fluorescence from 19 bands has been studied.²³ Low pressure lifetimes and fluorescence quantum yields from single vibronic levels of S_1 have been measured.²⁴⁻²⁶ Several notations have been used in labeling the ground state vibrations of *p*-DFB. We use the standard

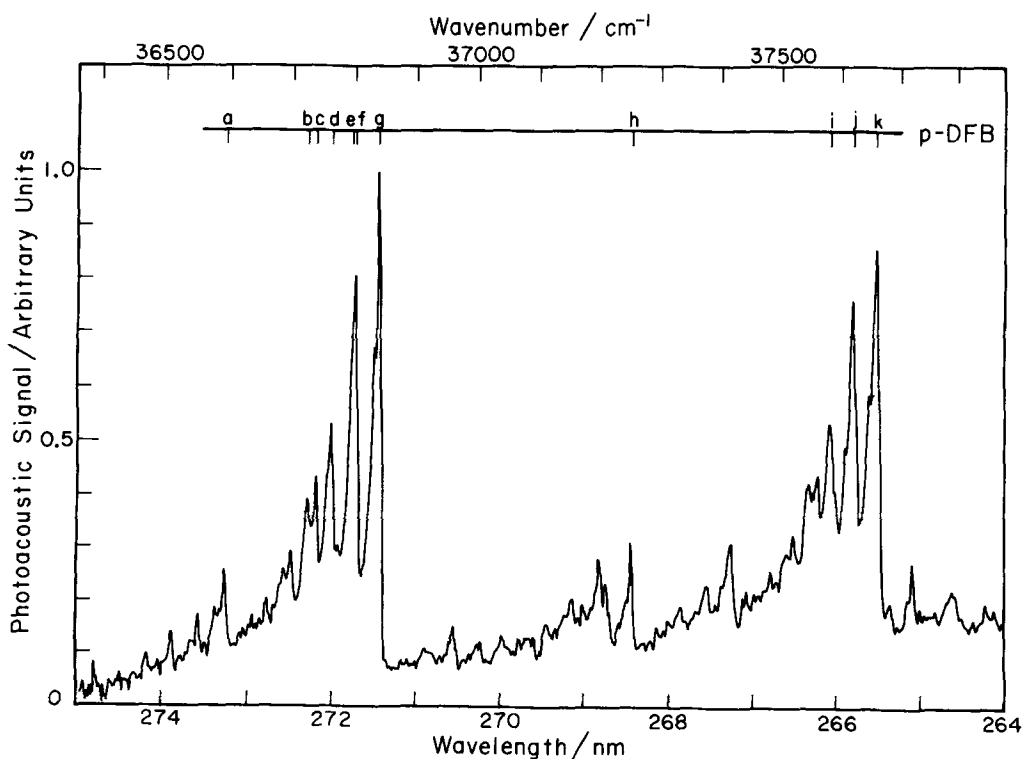


FIG. 4. Pulsed photoacoustic spectrum of a portion of the $\tilde{X}^1A_{1g} \rightarrow \tilde{A}^1B_{2u}$ transition in *p*-difluorobenzene. The sample consisted of 0.022 Torr *p*-difluorobenzene and 3.32 Torr helium. The photoacoustic signal has been corrected for the variation of incident laser pulse energy with wavelength. The vibronic bands labeled by the letters *a* through *k* are also listed in Table I. Each letter designates the following vibronic transitions: *a*— 8_1^1 , *b*— 30_3^3 , *c*— 17_1^1 , *d*— 30_2^2 , *e*— 27_1^1 , *f*— 30_1^1 , *g*— 0_0^0 , *h*— 6_0^1 , *i*— $5_0^1 30_2^2$, *j*— $5_0^1 30_1^1$, *k*— $5_0^1 (6_0^2)$. The symbol N_1^1 is defined in the text.

TABLE I. Observed vibronic transitions in the p -DFB $S_1(\bar{A}^1B_{2u})$ photoacoustic spectrum.

| Designation in Fig. 4 | Vibronic band assignment ^a | Transition energy (cm ⁻¹) ^a |
|-----------------------|---|--|
| a | 8 ₁ ¹ | 36 594 |
| b | 30 ₃ ⁰ | 36 726 |
| c | 17 ₁ ¹ | 36 740 |
| d | 30 ₂ ² | 36 764 |
| e | 27 ₁ ¹ | 36 797 |
| f | 30 ₁ ¹ | 36 802 |
| g | 0 ₀ ⁰ | 36 840 |
| h | 6 ₀ ¹ | 37 248 |
| i | 5 ₀ ¹ 30 ₂ ² | 37 583 |
| j | 5 ₀ ¹ 30 ₁ ¹ | 37 621 |
| k | 5 ₀ ¹ (6 ₀ ¹) ^b | 37 659 |

^aFrom Refs. 22 and 23.

^bFermi resonance mixes the 5¹ and 6² vibrational levels. The transition probability is predominantly derived from the 5¹ level.

Mulliken convention²⁷ for mode number designation in this paper, which is also used in Ref. 21. Transitions between vibronic levels in the ground electronic state and S_1 are denoted by N_i^j , where N is the number designating the mode involved and i and j are the number of quanta in mode in the ground and excited electronic states, respectively.

Figure 4 shows a photoacoustic spectrum of p -DFB produced by scanning the PUMP laser (no DUMP present). It agrees with the previous spectra obtained by other techniques.^{22,23} Assignments of the stronger transitions are given in Table I. In addition to the strong 0–0 band at 271.44 nm, the p -DFB spectrum consists predominantly of progressions in ν_5 and ν_3 , plus sequences associated with members of these progressions.²³ The 6₀¹ band is the strongest observed absorption involving quantum changes in modes other than ν_5 and ν_3 .²³ Single vibronic level fluorescence studies have identified the transition labeled k in Fig. 2 as involving excitation from the ground vibrational state to an excited state consisting of a Fermi resonance between states 5¹ and 6²,²³ with 5 contributing most of the transition intensity.

B. Results

Figure 5 shows a photoacoustic SEP spectrum of p -DFB produced by exciting the strong transition to the 5¹ and 6² resonant levels at 37 659 cm⁻¹ with the PUMP laser and scanning the DUMP laser from 286 to 284 nm. The figure shows three scans taken with different delay times between the PUMP and DUMP pulses. When the DUMP pulse occurs 20 ns before or 38 ns after the PUMP pulse, no change in photoacoustic signal is observed. When the DUMP pulse follows the PUMP pulse by 4 ns, the signal decreases by up to 10% at certain wavelengths, indicating that a SEP process is occurring at those wavelengths. The appearance of SEP only when DUMP immediately follows PUMP is consistent with the fluorescence lifetime of 10 ns observed for the 5¹ level of S_1 .^{24–26} Photoacoustic signal decreases as large as 15% have been observed. The fractional change depends critically on the spatial overlap of the two beams. No excited state absorption is observed for p -DFB

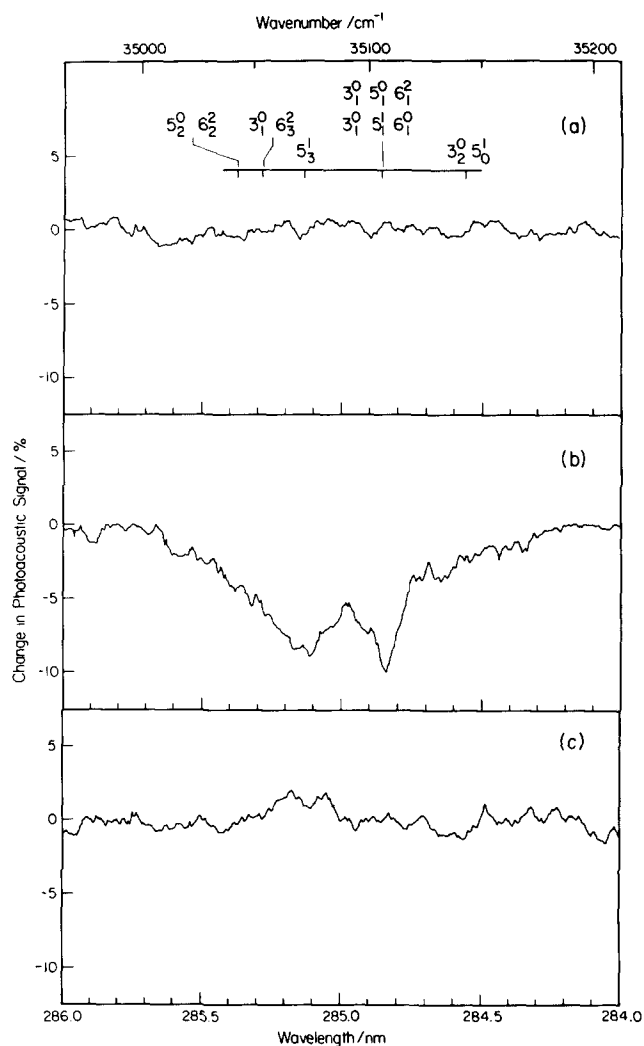


FIG. 5. Photoacoustic stimulated emission pumping spectrum of a 0.051 Torr sample of p -difluorobenzene obtained by pumping the 5₀¹ transition at 37 659 cm⁻¹ and scanning the DUMP pulse wavelength. The upper and lower abscissae give the photon energy and wavelength of the DUMP pulse. The ordinates give the percent change in photoacoustic signal due to the stimulated emission process. The transition labels refer to transitions induced by the DUMP pulse. The notation is described in the text. (a) The DUMP pulse precedes the PUMP pulse by 20 ns. (b) The DUMP pulse occurs 4 ns after the PUMP pulse. (c) The DUMP pulse occurs 38 ns after the PUMP pulse. In each spectrum the signal shown is the difference in photoacoustic signal produced by the PUMP pulse alone and the PUMP plus DUMP pulses. This difference signal has been corrected for variations in the DUMP laser pulse energy during the scan.

for the DUMP wavelengths used.

The SEP transitions observed in the 4 ns delay spectrum of Fig. 5 are easily assigned by considering the p -DFB single vibronic level fluorescence spectra and ground state fundamentals given in Ref. 23. In absorption and emission, the Franck–Condon factors allow large changes in vibrational quantum numbers for only modes ν_3 and ν_5 .²³ Quantum number changes for ν_6 are limited to ± 1 .²³ Changes in quantum numbers in other modes produce transitions which are weaker by an order of magnitude. Table II lists the possible ground electronic state vibrational levels which, according to Franck–Condon arguments, are expected to be most intense in fluorescence from the 5¹ or 6² levels populated by

TABLE II. *p*-DFB vibrational levels populated by stimulated emission pumping.

| Vibrational band | Vibrational energy (cm ⁻¹) | Predicted DUMP pulse transition energies ^a (cm ⁻¹) | Observed DUMP pulse transition energies ^a (cm ⁻¹) |
|--|--|---|--|
| 3 ₂ 5 ₀ | 2515 ^b | 35 144 | d |
| 3 ₁ 5 ₁ 6 ₁ | 2565 ^b | 35 094 | 35 108 |
| 5 ₃ | 2595 ^b | 35 064 | 35 073 |
| 3 ₁ 6 ₃ | 2604 ^c | 35 055 | d |
| 5 ₂ 6 ₂ | 2615 ^c | 35 044 | d |

^a Using a PUMP photon energy of 37 659 cm⁻¹.

^b Determined from 0-0 fluorescence data of Ref. 23.

^c Determined from ground electronic state vibrational frequencies of Ref. 23. Anharmonicity was not included.

^d Transition is present, but as a broad unresolved feature.

the PUMP laser. Each expected fluorescent transition is detected as a decrease in photoacoustic signal caused by SEP, although some transitions appear only as unresolved shoulders on the rotational envelopes of stronger transitions. The agreement between predicted and observed transition energies for the 3₁5₁6₁ and 5₃ levels is within expectations, considering the ± 5 cm⁻¹ accuracy of the fluorescence data²³ and the difference in excitation bandwidth (28 cm⁻¹ for fluorescence vs ≤ 1 cm⁻¹ for SEP).²⁸ The relative SEP intensities agree well with the resolved fluorescence spectrum intensities after exciting the 5¹ level.²³

Figure 6 shows a time resolved photoacoustic spectrum of *p*-DFB obtained by varying the relative time between the PUMP and DUMP pulses, while holding their respective photon energies constant at 37 659 and 35 108 cm⁻¹, respectively. This excites the 5¹ and 6² levels of S₁ and stimulates emission down to the 3₁5₁6₁ level of the ground electronic state. The time dependence of the SEP effect detected as a

decrease in photoacoustic signal is consistent with the 10 ns fluorescence lifetime²⁴⁻²⁶ of the 5¹ level of S₁ mentioned previously, if the laser pulse widths are taken into account.

The wavelength and time dependence of the *p*-DFB SEP signal detected by the photoacoustic effect provide evidence of the accuracy and usefulness of this new technique for monitoring SEP.

V. PHOTOACOUSTIC DETECTION OF EXCITED STATE ABSORPTION IN ANILINE

In this section the ability to detect excited state absorption, in contrast to stimulated emission, is demonstrated briefly by some data on aniline. A more detailed description of this work is presented elsewhere.⁸

Figure 7 shows a time-resolved photoacoustic spectrum of aniline obtained in a similar manner to that of the *p*-DFB spectrum of Fig. 6. In this case a 0.378 Torr sample of aniline is used and the PUMP and DUMP photon energies are 34 032 cm⁻¹ and 18 797 cm⁻¹, respectively. The PUMP pulse energy is 5.4 μJ, and the DUMP pulse energy is 6.5 mJ. Under these conditions the PUMP pulse excites the S₀→S₁ 0-0 transition^{29,30} and the DUMP pulse excites no resonant transitions from the ground state. In addition, it does not stimulate emission from S₁,³¹ and may possibly excite aniline from S₁ up to higher excited singlet states observed in vacuum UV absorption studies.³²⁻³⁴ In this case it is more appropriate to relabel the DUMP pulse as the TRANSFER pulse.⁸

In the spectrum of Fig. 7 a large *increase* in photoacoustic signal of up to 70% is observed when the TRANSFER pulse follows the PUMP one by 0 to 20 ns. When it is delayed longer than 20 ns, the signal decreases to a level that is still 20% higher than when it precedes the PUMP pulse. The fluorescence lifetime of the ground vibrational level of S₁ is approximately 8 ns,³⁵⁻³⁷ and therefore the large increase

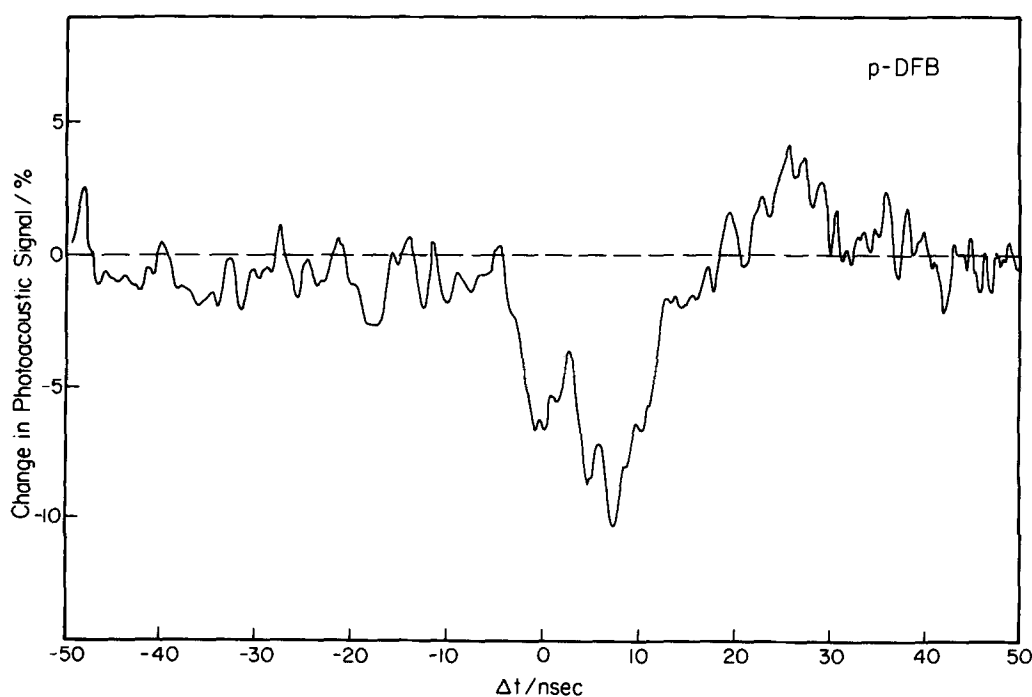


FIG. 6. Time-resolved stimulated emission pumping photoacoustic spectrum of a 0.051 Torr sample of *p*-difluorobenzene. The PUMP pulse excited the 5₀ transition of 37 659 cm⁻¹. The DUMP pulse stimulated emission out of the 5¹-6² resonant levels down to the 3₁5₁6₁ level. The spectrum was generated by scanning the delay between the PUMP and DUMP pulses. The abscissa gives the time delay between the two pulses, $\Delta t = t_{\text{DUMP}} - t_{\text{PUMP}}$. The ordinate gives the percent change in photoacoustic signal due to the stimulated emission process. The photoacoustic signal has not been corrected for time variations in the PUMP or DUMP pulse energies.

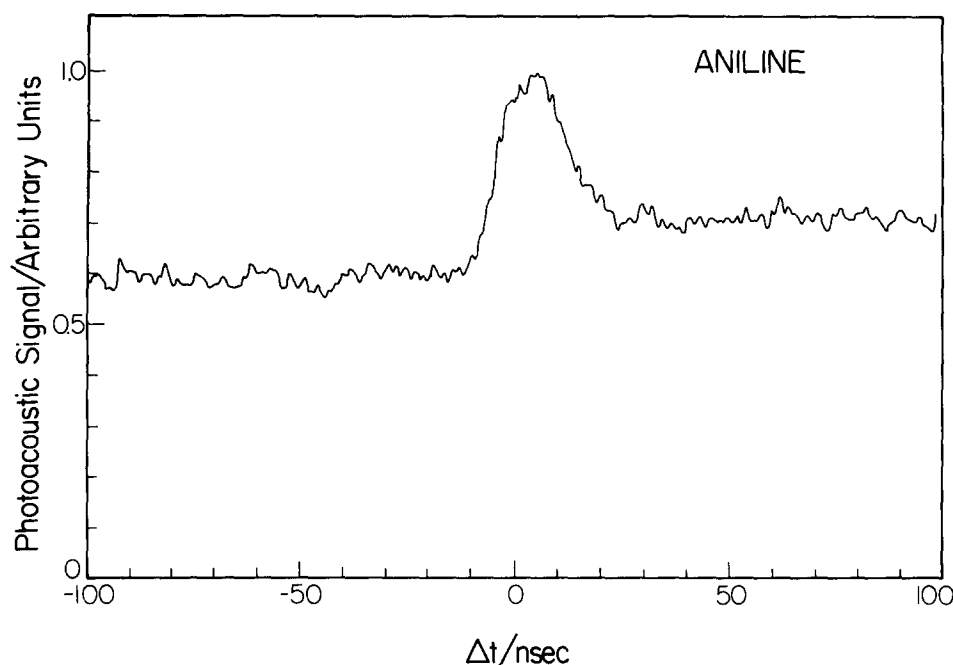


FIG. 7. Time-resolved pulsed photoacoustic spectrum of a 0.378 Torr sample of aniline. The PUMP photon excites the S_0 to S_1 0-0 transition at $34\,032\text{ cm}^{-1}$. The DUMP photon energy is $18\,797\text{ cm}^{-1}$. The spectrum was generated by scanning the time delay between the PUMP and DUMP pulses. The abscissa gives the time delay between the two pulses, $\Delta t = t_{\text{DUMP}} - t_{\text{PUMP}}$. The photoacoustic signal has not been corrected for variations in the PUMP or DUMP pulse energies.

from 0 to 20 ns delay results from excitation of the singlet state by the TRANSFER pulse. The longer apparent lifetime and increased signal for $\Delta t < 0$ are a result of the width of the PUMP and TRANSFER pulses and jitter in time delay generation. The increase in signal for delays longer than 20 ns most likely results from absorption from a long-lived triplet state produced by intersystem crossing.^{8,38}

VI. CONCLUSIONS

The results presented for *p*-DFB clearly demonstrate the sensitivity of the photoacoustic technique for monitoring SEP processes. The actual population transfer produced in these experiments was small due to the low pulse energy of the PUMP pulse. Increasing the PUMP pulse energy (which is not possible with the present equipment since the N_2 laser is already operated at its maximum power) should enhance the results reported here because of the increased signal to noise ratio.

The ability to detect excited state absorption, as demonstrated by the aniline study, and to distinguish that effect from SEP by simply monitoring the sign of the change in the photoacoustic signal, makes this technique an attractive alternative to the fluorescence detection method. The simplicity of photoacoustic detection compared with the PROBE laser-induced-fluorescence technique should also be emphasized.^{2,4,5}

The two-color time-resolved photoacoustic spectroscopy technique demonstrated here is a powerful tool for excited state spectroscopy. The results on *p*-DFB and aniline⁸ demonstrate its ability to determine single vibronic level lifetimes, detect gas phase excited state absorption from both singlet and triplet states, and also monitor SEP processes. By using an amplified intensity picosecond laser, the temporal resolution could easily be extended to the picosecond regime.

¹C. Kittrell, E. Abramson, J. L. Kinsey, S. A. McDonald, D. E. Reisner, R. W. Field, and D. H. Katayama, *J. Chem. Phys.* **75**, 2056 (1981).

²W. D. Lawrence and A. E. W. Knight, *J. Chem. Phys.* **76**, 5637 (1982).

³D. E. Reisner, P. H. Vaccaro, C. Kittrell, R. W. Field, J. L. Kinsey, and H. -L. Dai, *J. Chem. Phys.* **77**, 573 (1982).

⁴W. D. Lawrence and A. E. W. Knight, *J. Chem. Phys.* **77**, 570 (1982).

⁵W. D. Lawrence and A. E. W. Knight, *J. Phys. Chem.* **87**, 389 (1983).

⁶A. Schultz, H. W. Cruse, and R. N. Zare, *J. Chem. Phys.* **57**, 1354 (1972).

⁷R. N. Zare and P. J. Dagdigan, *Science* **185**, 739 (1974).

⁸D. J. Moll, G. R. Parker, Jr. and A. Kuppermann *J. Chem. Phys.* **80**, 4808 (1984).

⁹(a) M. G. Rockley and J. Paul Devlin, *Appl. Phys. Lett.* **31**, 24 (1977); (b) G. G. Yee and D. S. Klinger, *J. Phys. Chem.* **87**, 1887 (1983); (c) M. Bernstein, L. J. Rothberg, and K. S. Peters, in *Picosecond Phenomena III*, Springer Series in Chemical Physics Garmish-Partenkirchen, Federal Republic of Germany, June 16-18, 1982 (Springer, New York, 1982), Vol. 23, pp. 112-115.

¹⁰Moletron Corporation, 177 N. Wolfe Road, Sunnyvale, California 94086.

¹¹Laser Precision Corp., 1231 Hart Street, Utica, New York 13502.

¹²R. A. Keller, R. Engleman, Jr., and B. A. Palmer, *Appl. Opt.* **19**, 836 (1980).

¹³*Optoacoustic Spectroscopy and Detection*, edited by Yoh-Han Pao (Academic, New York, 1977).

¹⁴A. Rosencwaig, *Photoacoustics and Photoacoustic Spectroscopy* (Wiley, New York, 1980).

¹⁵G. A. West, D. R. Seibert, and J. H. Barrett, *J. Appl. Phys.* **51**, 2823 (1980).

¹⁶Knowles Electronics, Inc., 3100 N. Mannheim Rd., Franklin Park, Illinois 60131.

¹⁷J. H. S. Green, *Spectrochim. Acta. Part A* **26**, 15603 (1970).

¹⁸M. J. Robey and E. W. Schlag, *Chem. Phys.* **30**, 9 (1978).

¹⁹C. D. Cooper, *J. Chem. Phys.* **22**, 503 (1954).

²⁰S. N. Thakur and N. L. Singh, *Indian J. Pure Appl. Phys.* **7**, 765 (1969).

²¹Y. Udagawa, M. Ito, and S. Nagakura, *J. Mol. Spectrosc.* **36**, 541 (1970).

²²T. Cvitaz and M. J. Hollas, *Mol. Phys.* **18**, 793 (1970).

²³R. A. Coveleskie and C. S. Parmenter, *J. Mol. Spectrosc.* **86**, 86 (1981).

²⁴C. Guttman and S. A. Rice, *J. Chem. Phys.* **61**, 661 (1974).

²⁵L. J. Volk and E. K. C. Lee, *J. Chem. Phys.* **67**, 236 (1977).

²⁶D. Phillips, M. G. Rockett, and M. D. Swords, *Chem. Phys.* **38**, 301 (1979).

²⁷R. S. Mulliken, *J. Chem. Phys.* **23**, 1997 (1955).

²⁸It appears that the calculated positions of the $3^2_0 5^1_1 0^0_1$ sequence shown in Fig. 6 of Ref. 24 are too high by 858 cm^{-1} , the ν_3 fundamental frequency. Also the 0-0 single vibronic level fluorescence of the S^0_3 transition is dis-

placed 2595 cm^{-1} from 0_0^0 fluorescence, compared to the calculated value of 2574 cm^{-1} , indicating the possibility of perturbations of this level. These two clarifications bring the assignments of Ref. 24 and this paper into agreement.

²⁹N. Ginsberg and F. A. Matsen, *J. Chem. Phys.* **13**, 167 (1945).

³⁰J. C. D. Brand, D. R. Williams, and T. J. Cook, *J. Mol. Spectrosc.* **20**, 359 (1966).

³¹M. Quack and M. Stockburger, *J. Mol. Spectrosc.* **43**, 87 (1972).

³²K. Kimura, H. Tsubomura, and S. Nagakura, *Bull. Chem. Soc. Jpn.* **37**, 1336 (1964).

³³K. Kimura and S. Nagakura, *Mol. Phys.* **9**, 177 (1965).

³⁴K. Fuke and S. Nagakura, *J. Mol. Spectrosc.* **64**, 139 (1977).

³⁵J. Von Weissenhoff and F. Kraus, *J. Chem. Phys.* **54**, 2387 (1971).

³⁶W. R. Wave and A. M. Garcia, *J. Chem. Phys.* **61**, 187 (1974).

³⁷R. Scheps, D. Florida, and S. A. Rice, *J. Chem. Phys.* **61**, 1730 (1974).

³⁸K. C. Cadogan and A. C. Albracht, *J. Phys. Chem.* **73**, 1868 (1969).